EPR and ENDOR Investigations of a Cholestane Spin Probe in Liquid Crystals

B. Kirste
Institut für Organische Chemie, Freie Universität Berlin

Z. Naturforsch. **42 a,** 1296–1304 (1987); received August 8, 1987

A detailed ENDOR study of anisotropic proton hyperfine shifts in the nitroxide spin probe 3-doxylcholestane (CSL) in liquid-crystalline solution is described. The data are interpreted by means of theoretically calculated proton hyperfine tensors (McConnell-Strathdee-Derbyshire treatment), providing an independent check of the ordering matrix. The orientational order and the dynamic behavior of the nematic and smectic phases of the liquid crystals (40,6), (50,6), and 8CB are investigated by EPR using CSL and phenalenyl as spin probes.

Key words: EPR, ENDOR, liquid crystal, order parameters, smectic phase

Introduction

The investigation of orientational order and molecular motion in liquid crystals by EPR spectroscopy using suitable paramagnetic spin probes as reporter molecules is a well established method [1–3]. Nitroxide radicals with elongated, rod-like shape have found widespread use for this purpose since they are chemically stable and their EPR spectra are easily interpreted and allow reasonable conclusions with respect to the properties of the liquid-crystalline solvent [4–10]. It has been demonstrated that the order parameters of such spin probes – as determined from measured hyperfine splittings and g values – are proportional to the order parameters of the liquid crystals [11] and, in fact, similar in absolute magnitude. EPR lineshape studies of molecular dynamics, however, are faced with several difficulties. Thus, slow tumbling of the spin probes in low-temperature nematic and smectic phases requires the application of a sophisticated theoretical treatment for lineshape analyses [7, 12]. Moreover, the linewidths are affected by inhomogeneities of the sample and imperfect alignment of the director, and unresolved proton hyperfine splittings give rise to inhomogeneous line broadening.

Whereas the proton hyperfine splittings of typical nitroxide spin probes dissolved in viscous liquid crystals cannot be extracted from EPR spectra, this can be achieved by means of ENDOR (electron nuclear double resonance) spectroscopy. The application of ENDOR for unravelling isotropic and anisotropic hyperfine interactions in different types of radicals dissolved in smectic phases has been demonstrated in previous papers [13–15]. In the present paper a detailed ENDOR investigation of the cholestane spin probe 4′,4′-dimethylspiro(5α-cholestane-3,2′-oxazolidine)-N-oxyl (**CSL**) in liquid crystals is reported. The isotropic hyperfine couplings of this radical have already been determined by EPR [16], but the anisotropic contribution also operative in liquid-crystalline solution is quite considerable. Furthermore, EPR studies of this radical in several liquid crystals exhibiting nematic and various smectic phases (S_A, S_B, S_C, S_F, and S_G) will be presented, namely 4-cyano-4′-octylbiphenyl (**8CB**), N-(4-butoxybenzylidene)-4-hexylaniline (**40,6**), and N-(4-pentyloxybenzylidene)-4-hexylaniline (**50,6**). The main emphasis is given to an analysis of order parameters and phase transitions, whereas the temperature and angular dependence of the EPR linewidths will be discussed in a more phenomenological manner.

Experimental

Preparation of Samples

The liquid crystal **40,6** was synthesized by condensing equimolar quantities of 4-butoxybenzaldehyde and 4-hexylaniline [17], **8CB** was prepared according

* Reprint requests to Priv.-Doz. Dr. B. Kirste, Institut für Organische Chemie, Freie Universität Berlin, Takustraße 3, D-1000 Berlin 33, Germany.

0932-0784 / 87 / 1100-1296 $ 01.30/0. – Please order a reprint rather than making your own copy.

to [18], and **50,6** was a gift from Prof. G. Koßmehl, and the **CSL** spin probe was purchased from Aldrich. Phase transitions of the liquid crystals in °C, **8CB:** K 21 S_A 34 N 41 I, **40,6**: K 26 S_B 47.3 S_A 54.7 N 76.9 I, and **50,6**: K 32.5 S_G 40.2 S_F 43.0 S_B 51.3 S_C 52.8 S_A 61.2 N 73.0 I.

For EPR and ENDOR investigations, solutions of the spin probe ($10^{-3} - 10^{-4}$ M) in the liquid crystals were prepared in thin-walled cylindrical Pyrex sample tubes (3.3 mm o.d., 2.8 mm i.d.). The samples were thoroughly mixed and deoxygenated by warming them in a bath until the isotropic phase was formed and flushing with purified nitrogen. Radical concentrations were checked by comparing the second integral of the digitized EPR spectrum with that of a reference sample of known concentration. Oriented samples of smectic phases were obtained by slowly cooling the mesogen from the nematic phase in a strong magnetic field (ca. 1 T).

Instrumentation

EPR, ENDOR and TRIPLE spectra were recorded on a Bruker ER 220D EPR spectrometer equipped with a Bruker cavity (ER 200 ENB) and laboratory-built NMR facilities described elsewhere [19]. The spectrometer was interfaced to a minicomputer (HP 1000/A600) used for controlling the scan oscillator and the rf power (which was kept constant over the frequency range) in ENDOR experiments in addition to data acquisition and handling and storage of the spectra. EPR spectra were accumulated by using a Nicolet 1170 signal averager employing 1–4 K data points and afterwards transferred to the minicomputer. The spectrometer was stabilized by means of a field-frequency lock (Bruker ER 033). The temperature of the sample was adjusted by using a temperature control unit Bruker VT-1000 and checked by means of a thermocouple.

Results and Discussion

ENDOR Study of CSL in Isotropic Solution

The isotropic hyperfine interactions in the nitroxide spin probe 3-doxylcholestane (**CSL**) were first investigated in toluene by EPR, ENDOR, and TRIPLE resonance. The ^{1}H ENDOR spectrum exhibits four line pairs corresponding to hyperfine coupling constants of 2.83, 2.06, 1.70, and ca. 0.4 MHz (toluene, 220 K). The signals belonging to the smallest coupling are much broader and less intense than the others. Relative signs of the coupling constants were determined by means of general TRIPLE resonance [20], see Fig. 1 (left). Clearly the sign of the largest coupling is opposite to that of the next two. Moreover, the weak signals near the free proton Larmor frequency are shifted on pumping one of the outer resonances. Hence there are actually two line pairs with coupling constants of opposite sign and slightly different magnitude; the data are collected in Table 1.

^{14}N ENDOR signals could be observed at higher temperatures (e.g., toluene, 270 K), see Fig. 1 (right). The lines are centered about half the ^{14}N coupling constant ($a_N = 40.23$ MHz). The intensities of the two signals are different and depend on the field setting, but the cross-relaxation effects responsible for this behavior are not very pronounced (amplitude ratio of 1.5, dominant W_{X2}-process) [21]. However, also the ^{1}H ENDOR signal intensities are slightly influenced by this effect at this temperature, allowing the determination of the signs of the coupling constants relative to that of the ^{14}N coupling constant (CRISP technique [22, 23]). Since the latter can safely be assumed to be positive, all signs are now determined in an absolute sense (Table 1).

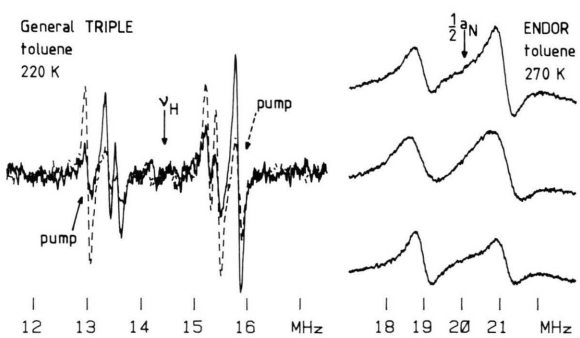

Fig. 1. *Left:* General TRIPLE spectra (^{1}H) of **CSL** in toluene (220 K). The pump frequencies are denoted by arrows (mw power 100 mW, rf power 60 W scan and 300 W pump). *Right:* ^{14}N ENDOR spectra of **CSL** in toluene (270 K) obtained with different field settings (top: low field, center: center field, bottom: high field; mw power 100 mW, rf power 210 W corresponding to $B_{rf} \approx$ 0.6 mT in the rotating frame, frequency modulation amplitude 200 kHz).

Since the ENDOR spectra do not provide reliable information on the numbers of contributing nuclei, the multiplicities were determined by means of computer simulations of the EPR spectrum. Because optimum EPR and ^{1}H ENDOR spectra are obtained at different temperatures, a fit procedure using the ENDOR data as starting values has been employed (program NOFIT [24]). The simulation takes M_I-dependent linewidths into account, see Fig. 2 (left). It stands to reason that coupling constants less than the linewidth of about 0.02 mT and their multiplicities cannot be determined reliably by this procedure. The three largest proton coupling constants are in agreement with those reported previously [16].

Table 1. Isotropic hyperfine coupling constants and hyperfine shifts (in MHz) of 3-doxylcholestane [a].

Position	a toluene 220 K	a (**50,6**) 330 K	Δa_{exp} (**50,6**) 330 K	Δa_{calc} [b]
^{14}N	+40.23 [c]	+40.63 [d]	−20.54 [d]	−21.3
a (1 H, δ, eq)	+2.83	+2.82	+0.78	+0.78
b (2 H, γ, ax)	−2.06	−2.08	+2.52	+2.90
c (2 H, γ, eq)	−1.70	−1.67	+0.23	+0.23
d (2 H, δ, ax)	+0.55	+0.55	+0.89	+1.01
e (6 H, Me)	−0.33	−0.42	+0.56	+0.27 [e]
		±0.10	±0.72 (?)	[f]
		±0.10	±0.22 (?)	
g-value		2.00580	+0.00039	

[a] ENDOR measurements, accurate within ±0.01 MHz. For the labelling of positions, see Figure 4.
[b] Calculated with tensor data from Table 2 and the following order parameters: $O_{yy} = 0.80$, $O_{xx} = O_{zz} = -0.40$.
[c] At 270 K.
[d] EPR measurement.
[e] Average for three methyl protons in a single conformation.
[f] Calculated shift for the γ protons in the oxazolidine ring (position 5′): −1.39 MHz.

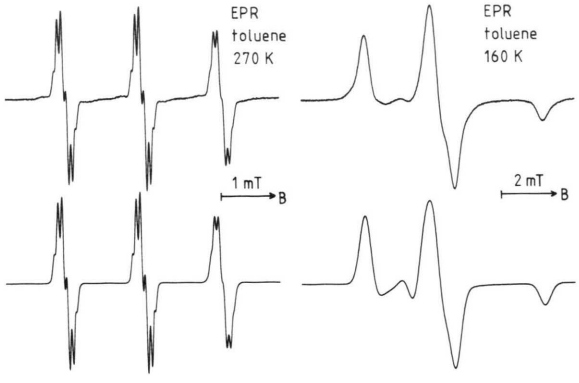

Fig. 2. *Left:* EPR spectrum of **CSL** in toluene (270 K; top) and computer simulation (bottom; coupling constants (in MHz): 40.06 (1 N), 2.79 (1 H), 2.01 (2 H), 1.70 (2 H), 0.59 (2 H), and 0.32 (6 H); Lorentzian peak-to-peak linewidth parameters (in mT, cf. (6): $A = 0.020$, $B = -0.006$, and $C = 0.008$). *Right:* EPR spectrum of **CSL** in glassy toluene (160 K; top) and computer simulation (bottom; $g_{xx} = 2.0091$, $g_{yy} = 2.0061$, $g_{zz} = 2.0023$, $A_{xx} = A_{yy} = 14.6$ MHz, $A_{zz} = 91.4$ MHz, linewidth 0.47 mT (full width at half height, Gaussian shape)).

The principal components of the ^{14}N hyperfine and g tensors were extracted from an EPR spectrum taken in glassy toluene, see Fig. 2 (right). A computer simulation is also depicted in Figure 2. The data for the x, y components are not very accurate because of the poor resolution of the central part of the spectrum ($A_{xx} \approx A_{yy} = 14.6$ MHz, $A_{zz} = 91.4$ MHz, $g_{xx} = 2.0091$, $g_{yy} = 2.0061$, and $g_{zz} = 2.0023$; see also [25]).

ENDOR Study of **CSL** *in Smectic Phases*

Anisotropic proton hyperfine components cannot be extracted from EPR spectra taken in glassy or liquid-crystalline solution because the proton splittings are not resolved. However, well-resolved ^{1}H ENDOR spectra can be obtained in oriented smectic phases. Figure 3 shows ^{1}H ENDOR spectra of 3-doxylcholestane in the smectic A phase of (**40,6**) for three different angles between the director and the static magnetic field. Obviously the proton hyperfine splittings are strongly angular dependent due to anisotropic contributions.

To a good approximation, the angular dependence of proton hyperfine splittings is given by

$$\bar{a}(\gamma) = \tilde{A}_\perp + (\tilde{A}_\parallel - \tilde{A}_\perp)\cos^2\gamma, \tag{1}$$

where

$$\tilde{A}_\parallel = \bar{a}(0°) = a + \Delta a, \tag{2}$$

$$\tilde{A}_\perp = \bar{a}(90°) = a - \Delta a/2. \tag{3}$$

The anisotropic hyperfine shifts Δa depend on the respective dipolar hyperfine tensor and the ordering matrix (vide infra). Equation (1) can be rewritten as

$$\bar{a}(\gamma) = a + \Delta a - \tfrac{3}{2}\Delta a \sin^2\gamma. \tag{4}$$

Thus, a plot of $\bar{a}(\gamma)$ vs. $\sin^2\gamma$ should be linear, and the determination of the isotropic coupling constant a and the anisotropic shift Δa is straightforward.

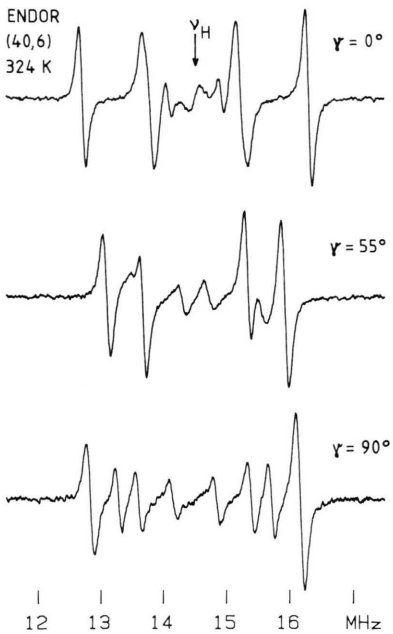

Fig. 3. ENDOR spectra of **CSL** in the smectic A phase of (**40,6**) taken at three different angles between the director and the static magnetic field (324 K, mw power 100 mW, rf power 100 W corresponding to $B_{rf} \approx 0.4$ mT in the rotating frame).

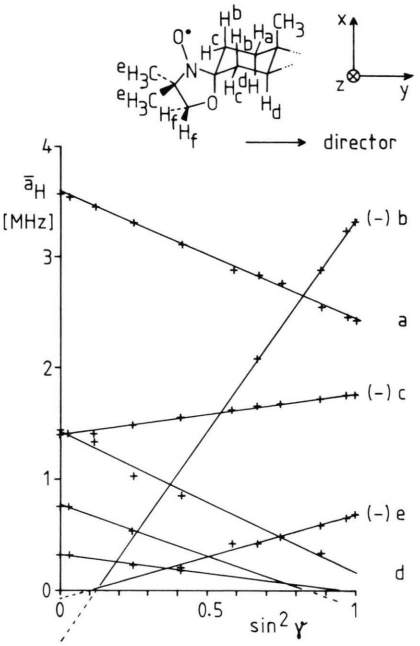

Fig. 4. Angular dependence of the observed proton hyperfine splittings of **CSL** in the smectic A phase of (**50,6**) at 330 K (ENDOR data). Note that some of the coupling constants (denoted by *b*, *c*, and *e*) actually have negative signs.

ENDOR spectra of **CSL** in the smectic A phase of (**50,6**) have been measured in angular steps of 10°. A plot of the observed hyperfine splittings is given in Figure 4. Although not all signals could be followed through the whole range of orientations due to overlap of lines, the analysis is unambiguous at least for the larger couplings. The results are collected in Table 1.

Attempts to record ^{14}N ENDOR spectra of **CSL** in liquid-crystalline solution did not succeed so far. Such measurements would be informative since they could provide ^{14}N quadrupole splittings as has been demonstrated for small nitroxide molecules [26]. However, voluminous nitroxide radicals such as **CSL** require solvents of low viscosity to achieve rotational correlation times short enough for a measurable ^{14}N ENDOR enhancement [27]. Actually weak ^{14}N ENDOR signals of **CSL** could be recorded in the isotropic phase of 4,4′-dimethoxyazoxybenzene (**PAA**) at 420 K, but clear-cut results could not be achieved in the nematic phase, the more so since the ^{14}N ENDOR signals are shifted into the proton region.

Interpretation of the Hyperfine Shifts

The anisotropic hyperfine shifts Δa observed in liquid-crystalline solution depend on the inner product of the traceless ordering matrix (elements O_{ij}) and the respective dipolar hyperfine tensor (elements A'_{ij}) [28]. In a principal axes system, one obtains

$$\Delta a = O_{yy} A'_{yy} + \tfrac{1}{3} (O_{zz} - O_{xx}) (A'_{zz} - A'_{xx}) , \tag{5}$$

assuming that the molecules are mainly aligned along the y axis (long molecular axis). (An analogous equation applies to the g tensor.) The ordering matrix of **CSL** can be determined from the nitrogen hyperfine and g tensors [25]. With tensor data from powder measurements (A'_{yy}(N) ≈ − 25.6 MHz, vide supra), $O_{yy} = 0.80$ is obtained for **CSL** in the smectic A phase of (**50,6**) (at 330 K; see Table 1) provided that $O_{xx} \approx O_{zz}$.

The proton hyperfine tensors are not directly accessible from the available experimental data, but they can be calculated according to the theory developed by McConnell and Strathdee [29] and equations for non-planar radicals given by Derbyshire [30] and by Pitzer et al. [31]; see also [28, 32].

Table 2. Spin populations and calculated dipolar hyperfine tensors [a] (in MHz) of 3-doxylcholestane.

Position	ϱ_π	A'_{xx}	A'_{yy}	A'_{zz}
^{14}N(N–O)	0.54	−24.3	−26.6	50.9
^{16}O(N–O)	0.46			
a (δ, *e q*)		−0.720	0.978	−0.258
b (γ, *a x*)		−2.744	3.627	−0.884
c (γ, *e q*)		−2.957	0.282	2.676
d (δ, *a x*)		−0.586	1.262	−0.676
e (Me, H-1)		0.670	0.110	−0.780
(Me, H-2)		−2.349	3.247	−0.898
(Me, H-3)		−0.174	−2.329	2.504
f (γ'(5'))		3.083	−1.742	−1.342

[a] Calculated according to McConnell and Strathdee [29] and Derbyshire [30] with structural data for 4',4'-dimethylspiro(cyclohexane-1,2'-oxazolidine)-N-oxyl [33]. The *y* axis is the long molecular axis (angle of 70° with the N–O bond axis), the *z* axis is parallel to the N,O p orbitals (cf. Fig. 4) [25].

For these calculations, the geometry of the radical and the spin density distribution must be known. Structural data for the relevant fragment of **CSL** have been taken from an X-ray study of the related radial 4',4'-dimethylspiro(cyclohexane-1,2'-oxazolidine)-N-oxyl [33]. The π spin population at the nitrogen atom was estimated from a comparison of the experimental hyperfine tensor data with a calculation using parameters given in [34], yielding $\varrho_\pi(\mathrm{N}) = 0.54$. The remaining π spin population is assumed to be localized at the oxygen atom of the nitroxyl group. The calculated dipolar hyperfine tensors are given in Table 2, and the calculated hyperfine shifts are collected in Table 1. Since the agreement with the experimental data is remarkably good, the assumptions about the ordering matrix are evidently justified.

EPR Study of Molecular Order in Liquid Crystals

A series of EPR spectra of **CSL** in the liquid crystal (**50,6**) taken at different temperatures is depicted in Figure 5. At 342 K, pure (**50,6**) forms a nematic phase. The **CSL** spin probe, however, is chiral and induces a cholesteric phase (concentration ca. $2 \cdot 10^{-3}$ M in this case). The helical twist gives rise to a distribution of local director orientations and hence a characteristic powder-type EPR spectrum is obtained [35, 36].

On lowering the temperature until a smectic A phase forms, an EPR spectrum with a complicated powder-type pattern due to a nonuniform director distribution is observed. However, a smectic A phase with a uniform director orientation has been obtained by cooling the sample slowly in an external magnetic field of 1 T (see Figure 5), because a strong magnetic field causes unwinding of the helical structure in an induced cholesteric phase [36]. Since the director of a smectic phase is not reoriented by a magnetic field (0.34 T in the EPR experiments), angular dependences can conveniently be studied. For instance, the observed nitrogen hyperfine splitting is strongly angular dependent.

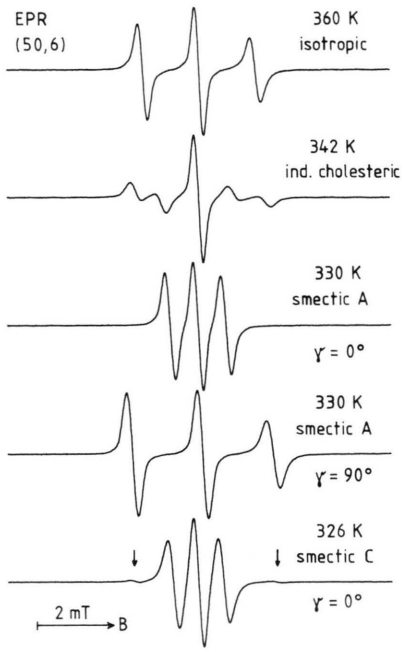

Fig. 5. EPR spectra of **CSL** in (**50,6**) at different temperatures. Note that at 342 K a cholesteric phase is induced by the chiral spin probe (concentration ca. $2 \cdot 10^{-3}$ M). The spectra in the smectic phases were recorded after cooling the sample in an external magnetic field of 1 T. Spectra taken in the smectic A phase (330 K) are shown with the director parallel and perpendicular to the magnetic field. Note the appearance of powder-type features in the smectic C phase.

In contrast to the smectic A phase, the single-crystal-type appearance of the EPR spectra is lost in the smectic C phase (326 K, see Figure 5). Since the director axis is tilted with respect to the normal of the smectic layers in a smectic C phase, a uniform director orientation cannot be achieved by the employed method of sample preparation (see Experimental; an alternative method is described in [8]). The powder-type lineshape remains essen-

tially unchanged in the smectic B, F, and G phases forming at still lower temperatures.

In order to estimate the degree of ordering in the liquid-crystalline phases, it was assumed that the order parameter $S^* = O_{yy}$ of the **CSL** solute molecules should be an appropriate measure for the order parameter of the mesophase. For the reasons discussed above, this applies only to the smectic A phase of (**50,6**). The order parameter S^* was calculated from the observed nitrogen hyperfine shift ($S^* \approx -\Delta a_N/25.6$ MHz, vide supra). For comparison, the disk-shaped molecule phenalenyl was used as spin probe in a second series of measurements. In the case of phenalenyl, the order parameter $S^* = -2 \cdot O_{zz}$ (the z axis represents the symmetry axis perpendicular to the molecular plane) should provide a lower limit of the order parameter of the mesophase [37].

The results are depicted in Figure 6. The order parameter S^* obtained with the phenalenyl probe shows the expected temperature dependence in the nematic and smectic A phases of (**50,6**), namely an increase in the nematic phase with decreasing temperature, a sharp increase at the phase transition to the smectic A phase and little change in the smectic A phase. It is noteworthy that the **CSL** probe achieves a much higher degree of ordering ($S^* \approx 0.8$) than the phenalenyl probe ($S^* \approx 0.6$) in the smectic A phase, probably because the **CSL** molecules are preferentially located in proximity to the aromatic portions of the solvent molecules, whereas the phenalenyl molecules are apparently expelled to the region of the flexible hydrocarbon chains.

At the phase transition to the smectic C phase, the order parameter S^* of the phenalenyl probe sharply decreases, obviously because of disorder introduced by the tilted phase structure. Since the phenalenyl molecule is highly mobile [37], site inequivalencies are averaged out and single-crystal-type spectra are obtained. S^* (phenalenyl) remains virtually constant in the smectic B phase and then decreases again in the smectic F phase. Thus, all phase transitions of (**50,6**) are clearly visible in a plot of S^* (phenalenyl) vs. temperature (see Fig. 6), whereas the absolute value of S^* (phenalenyl) is certainly much smaller than the "true" microscopic order parameter of the smectic phases. In contrast, a well-defined order parameter can hardly be extracted from the powder-type EPR spectra of **CSL**

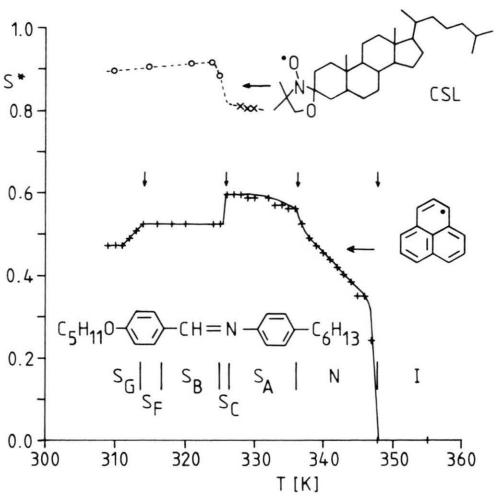

Fig. 6. Temperature dependence of the effective order parameter S^* (see text) of the two spin probes **CSL** and phenalenyl in the liquid crystal (**50,6**). Note that the phase transitions are clearly visible in the lower curve, S^* (phenalenyl).

in the low-temperature smectic phases (C to G). The values of S^* (**CSL**) included in Fig. 6 have been derived from the line separations of the three intense peaks; they do not show a significant temperature dependence ($S^* \approx 0.9$).

The results of EPR investigations of the liquid crystal (**40,6**) with the **CSL** spin probe are depicted in Fig. 7, showing the temperature dependences of the order parameter S^* (top) as well as the linewidth parameters B and C (bottom). The EPR linewidths (T_2^{-1}) were determined from computer simulations using a fit procedure (program NOFIT [24]), taking the proton hyperfine splittings (data from ENDOR measurements) and the M_I dependence into account,

$$T_2^{-1} = A + BM_I + CM_I^2 . \tag{6}$$

Whereas the linewidths increase in the isotropic phase with decreasing temperature due to increasing viscosity of the solvent and hence slower molecular tumbling, they decrease in the nematic and smectic mesophases. This decrease is due to the influence of molecular ordering, restricting the line-broadening effects of the modulation of anisotropic interactions by molecular motion. The discontinuities at the phase transitions (isotropic/nematic and nematic/smectic A) are probably caused by thermal gradients over the sample volume (coexistence of two phases).

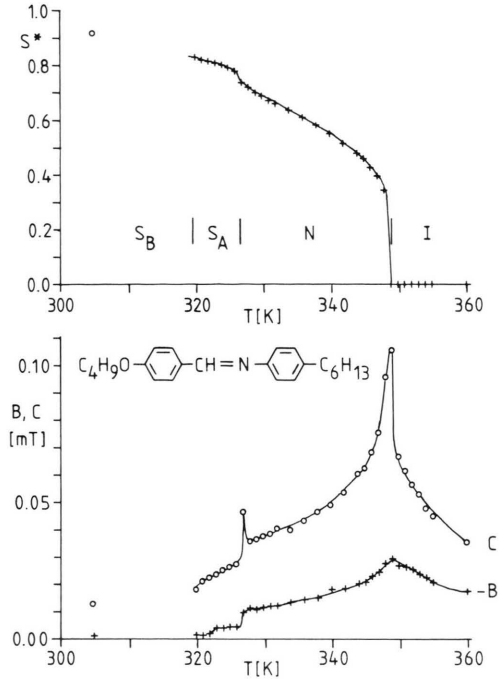

Fig. 7. Temperature dependence of the effective order parameter S^* (top) and the EPR linewidth parameters (bottom) of **CSL** in (**40,6**). The parameters B and C (cf. (6)) refer to Lorentzian peak-to-peak linewidths.

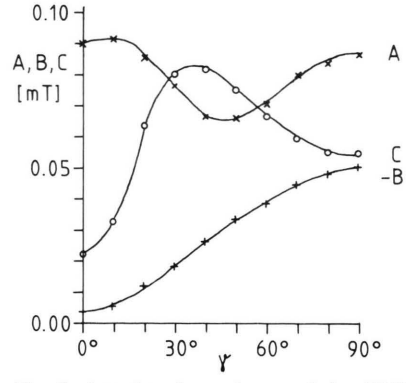

Fig. 8. Angular dependence of the EPR linewidth parameters A, B, and C of **CSL** in the smectic A phase of (**40,6**) at 324 K (cf. (6) and (7); the parameters refer to Lorentzian peak-to-peak linewidths).

Figure 8 shows a plot of the angular dependence of the linewidth parameters A, B, and C of **CSL** in the smectic A phase of (**40,6**). Whereas the parameter $-B$ increases monotonously from 0° to 90°, the value of C passes through a maximum at about 40°. Theory predicts the following angular dependence of the parameter B in the fast-tumbling limit:

$$B(\gamma) = B_0 + B_2 P_2(\cos\gamma) + B_4 P_4(\cos\gamma), \quad (7)$$

where $P_2(\cos\gamma)$ and $P_4(\cos\gamma)$ are Legendre polynomials; analogous equations apply to the parameters A and C [5, 38]. The parameters B_0, B_2, and B_4 in (7) depend on the dipolar hyperfine and g tensors, the orientational order parameters $\bar{P}_2$ (denoted S^* in the previous discussion) and $\bar{P}_4$ and the rotational correlation times τ_0 and τ_2. In principle, the higher order parameter $\bar{P}_4$ and the rotational correlation times can be determined by adjusting the parameters in (7) until agreement with the experimentally observed angular dependence is achieved. However, (7) is not strictly applicable to the case under study dealing with the slow tumbling region. Moreover, inhomogeneous linewidth contributions due to imperfect alignment of the director or director fluctuations should be taken into account. These effects are probably responsible for the observation of a pronounced maximum of the parameter C at intermediate angles ($\gamma \approx 40°$, see Figure 8). Since a detailed EPR lineshape study of the **CSL** probe in (**40,6**) has already been reported by Meirovitch and Freed [8], this topic will not be pursued further here. It should be noted, however, that the motion of the **CSL** probe in the smectic B phase of (**40,6**) is quite similar to that at the low-temperature end of the smectic A phase. Obviously this behavior does not correlate with the macroscopic viscosity of these phases.

Finally spin probe investigations of the liquid crystal 8CB shall be considered. For the **CSL** probe in the smectic A phase of 8CB the following data have been obtained (295 K): $a_N = 40.92$ MHz, $\Delta a_N = -18.52$ MHz, and $S^* = 0.72$. It is noteworthy that a similar order parameter has been found for the phenalenyl probe, namely $S^* = 0.68$ [37]. So in this respect the smectic A phase of **8CB** behaves quite differently from that of (**50,6**) which shows pronounced differences regarding the order parameters of these two probes (vide supra). Moreover, the linewidths in the EPR spectra of **CSL** in **8CB** are much larger than those observed in (**50,6**) or (**40,6**), see Figure 9. Thus, the parameters B and C are roughly three times as large as in (**40,6**) (smectic A or B phase), indicating a higher "microviscosity" in **8CB**. This peculiar behavior of **8CB** is probably related to the particular phase structure of its smectic A phase which exhibits an interdigitated

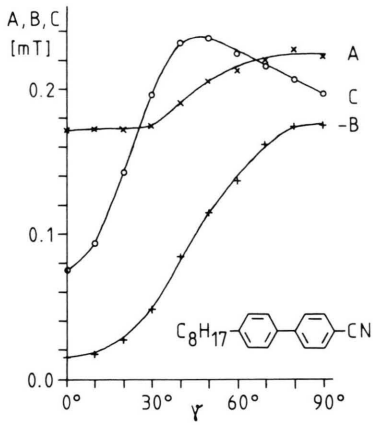

Fig. 9. Angular dependence of the EPR linewidth parameters of **CSL** in the smectic A phase of **8CB** at 295 K (cf. caption of Figure 8).

bilayer arrangement with a lamellar spacing of about 1.5 times the molecular length [39]. (A claim that the smectic A phase of **8CB** is reoriented by an external magnetic field [12] could not be confirmed in our laboratory, provided the measurements are performed well below the $N - S_A$ transition temperature.)

Conclusion

It has been demonstrated that the anisotropic proton hyperfine shifts of the widely used cholestane spin probe 3-doxylcholestane (**CSL**) can be obtained from ENDOR measurements in liquid-crystalline solution. These data provide further confirmation for the ordering matrix derived from nitrogen hyperfine and g shifts. Moreover, they allow proper simulations of the EPR spectra, taking the inhomogeneous line broadening by unresolved proton hyperfine splittings into account. This eliminates one of the problems encountered in EPR lineshape studies of molecular motion.

The investigation of molecular order in mesophases is certainly of particular interest in liquid-crystal research. While theories predict that a set of order parameters should adequately describe this phenomenon, it has become clear that experimental methods can only give approximate answers. Whereas ^{2}H NMR studies of deuterated liquid crystals yield accurate local order parameters [40], the EPR spin probe technique rather supplies *integral* order parameters, but it is an indirect method using solute molecules as reporters. This problem will be more serious in smectic or discotic phases than in nematic phases because they are not homogeneous on a microscopic level. Thus, the spin probe is likely to show a preference for a particular region, e.g., the highly ordered core or the less ordered side chains. In the present study it has been shown that two different spin probes, namely **CSL** and phenalenyl, give similar results regarding the order parameters in the smectic A phase of some liquid crystals (**8CB**), whereas quite different results are obtained for other liquid crystals (smectic A phases of (**40,6**) and (**50,6**)). Moreover, studies of the dynamic behavior of the **CSL** spin probe indicate that the microviscosities of smectic liquid crystals depend much more on the chemical structure than on the phase structure (e.g., S_A or S_B).

Acknowledgements

I wish to thank Mrs. M. Frühauf and Prof. Dr. G. Koßmehl (FU Berlin) for a sample of the liquid crystal (**50,6**) and Mr. J. Buchner for the preparation of (**40,6**). I am grateful to Prof. Dr. H. Kurreck for his support of this work. Financial support by the Deutsche Forschungsgemeinschaft (Schwerpunktprogramm „Thermotrope Flüssigkristalle") and the Fonds der Chemischen Industrie is gratefully acknowledged.

[1] L. J. Berliner (ed), Spin Labeling. Theory and Applications, Vol. 1, Academic Press, New York 1976.
[2] G. R. Luckhurst, in Liquid Crystals and Plastic Crystals, G. W. Gray and P. A. Winsor (eds.), Ellis Horwood, Chichester 1974, Vol. 2, Chapter 7.
[3] P. L. Nordio and U. Segre, in The Molecular Physics of Liquid Crystals, G. R. Luckhurst and G. W. Gray (eds.), Academic Press, London 1979, Chapters 16 and 19.
[4] G. R. Luckhurst and M. Setaka, Mol. Cryst. Liq. Cryst. **19,** 179 (1972).
[5] G. R. Luckhurst, M. Setaka, and C. Zannoni, Mol. Phys. **28,** 49 (1974).
[6] F. Pusnik and M. Schara, Chem. Phys. Lett. **37,** 106 (1976).
[7] K. V. S. Rao, C. F. Polnaszek, and J. H. Freed, J. Phys. Chem. **81,** 449 (1977).

[8] E. Meirovitch and J. H. Freed, J. Phys. Chem. **84,** 2459 (1980).
[9] N. V. S. Rao, V. G. K. M. Pisipati, P. V. Datta Prasad, and D. Saran, Z. Naturforsch. **40a,** 469 (1985).
[10] S. Mita and S. Kondo, Mol. Cryst. Liq. Cryst. **140,** 153 (1986).
[11] S. K. Ghosh, A. Ricchiuto, A. Panatta, and P. L. Indovina, Nuovo Cim. Soc. Ital. Fis., **D 7,** 825 (1986).
[12] W.-J. Lin and J. H. Freed, J. Phys. Chem. **83,** 379 (1979).
[13] B. Kirste, Chem. Phys. Lett. **64,** 63 (1979).
[14] B. Kirste, H. Kurreck, H.-J. Fey, Ch. Hass, and G. Schlömp, J. Amer. Chem. Soc. **101,** 7457 (1979).
[15] B. Kirste and H. Kurreck, Appl. Spectrosc. **34,** 305 (1980).
[16] T. B. Marriott, S. P. Van, and O. H. Griffith, J. Magn. Reson. **24,** 41 (1976).
[17] Z. G. Gardlund, R. J. Curtis, and G. W. Smith, in Liquid Crystals and Ordered Fluids, J. F. Johnson and R. S. Porter (eds.), Plenum Press, New York 1974, Vol. 2, p. 541.
[18] A. I. Pavlyuchenko, N. I. Smirnova, E. I. Kovshev, V. V. Titov, and G. V. Purvanetskas, Zh. Org. Khim. **12,** 1054 (1976); J. Org. Chem. USSR **12,** 1066 (1976).
[19] H. Kurreck, B. Kirste, and W. Lubitz, Angew. Chem. **96,** 171 (1984); Angew. Chem., Int. Ed. Engl. **23,** 173 (1984).
[20] R. Biehl, M. Plato, and K. Möbius, J. Chem. Phys. **63,** 3515 (1975).
[21] D. S. Leniart, J. C. Vedrine, and J. S. Hyde, Chem. Phys. Lett. **6,** 637 (1970).
[22] W. Lubitz and T. Nyrönen, J. Magn. Reson. **41,** 17 (1980).
[23] E. G. Janzen and U. M. Oehler, Chem. Lett. **1985,** 111.
[24] B. Kirste, J. Magn. Reson. **73,** 213 (1987).
[25] S. G. Carr, S. K. Khoo, G. R. Luckhurst, and C. Zannoni, Mol. Cryst. Liq. Cryst. **35,** 7 (1976).
[26] K. P. Dinse, K. Möbius, M. Plato, R. Biehl, and H. Haustein, Chem. Phys. Lett. **14,** 196 (1972).
[27] M. Plato, W. Lubitz, and K. Möbius, J. Phys. Chem. **85,** 1202 (1981).
[28] H. R. Falle and G. R. Luckhurst, J. Magn. Reson. **3,** 161 (1970).
[29] H. M. McConnell and J. Strathdee, Mol. Phys. **2,** 129 (1959).
[30] W. Derbyshire, Mol. Phys. **5,** 225 (1962).
[31] R. M. Pitzer, C. W. Kern, and W. N. Lipscomb, J. Chem. Phys. **37,** 267 (1962).
[32] B. Kirste, Magn. Reson. Chem. **25,** 166 (1987).
[33] D. Bordeaux and J. Lajzérowicz-Bonneteau, Acta Cryst. **B 30,** 2130 (1974).
[34] N. M. Atherton, Electron Spin Resonance, Ellis Horwood, Chichester 1973, p. 131.
[35] G. R. Luckhurst and H. J. Smith, Mol. Cryst. Liq. Cryst. **20,** 319 (1973); Mol. Phys. **29,** 317 (1975).
[36] G. Gottarelli, G. F. Pedulli, and C. Zannoni, Chem. Phys. **64,** 143 (1982).
[37] B. Kirste, Chem. Phys. Lett. **83,** 465 (1981).
[38] G. R. Luckhurst, M. Setaka, and R. N. Yeates, J. Magn. Reson. **42,** 351 (1981).
[39] G. W. Gray and J. E. Lydon, Nature, London **252,** 221 (1974); A. J. Leadbetter, J. L. A. Durrant, and M. Rugman, Mol. Cryst. Liq. Cryst. **34,** 231 (1977).
[40] J. W. Emsley and J. C. Lindon, NMR Spectroscopy using Liquid Crystal Solvents, Pergamon Press, Oxford 1975.